CrossMark

ORIGINAL ARTICLE

A new method for absolute datum transfer in seafloor control network measurement

Jianhu Zhao[1] · Yajing Zou[1] · Hongmei Zhang[2] · Yongting Wu[3] · Shouchuan Fang[4]

Abstract To decrease the time consumption and the labor intensity in the absolute datum transfer of traditional seafloor control network measurement, a new method, namely sailing-circle positioning method, is put forward in this paper. First, the traditional intersection positioning model is improved by considering the equivalent sound velocity profile error as an unknown parameter in the adjustment model. Second, the effect of geometric dilution of precision (GDOP) on positioning accuracy is analyzed. By seeking for the minimum of GDOP, it is concluded that the absolute datum transfer can achieve the highest accuracy in the condition of sailing along a circle relative to other sailing paths. Moreover, the optimal radius of the circle for the accurate datum transfer is also given out. Besides, the correlation between the accuracy of datum transfer and the sound velocity error in this method is analyzed. Finally, the new method was tested and verified by the experiments in Songhua lake with the water depth of 60 m and in South China sea with the water depth of 2000 m, respectively. These experiment results show that the new method can improve the accuracy and efficiency of traditional datum transfer method significantly.

1 Introduction

Seafloor control network plays an important role in the underwater acoustic positioning, such as the navigation service for unmanned underwater vehicles (UUV) or autonomous underwater vehicle (AUV), the monitoring of submarine building, crustal movement in seism fault. To keep the underwater measurement datum consistent with that on land and water surface, it is necessary to transfer horizontal and vertical datum from water surface to underwater in the geographic coordinate framework.

The absolute datum transfer is carried out by two steps in traditional measurement [1, 2]. First, the horizontal datum transfer is done by double-three-pyramid method; second, the vertical datum transfer is fulfilled by four-leaf method combined with tide level of the measurement region. According to the measurement mechanism, double-three-pyramid method has the following defects which will decrease the accuracy and efficiency of the horizontal datum transfer [3, 4]: (1) to avoid the significant influence of sea current on the accuracy of datum transfer, multiple survey vessels or carriers are required to operate synchronously; (2) the accurate measurement distance depends strictly on SVPs, so it is necessary to measure SVPs in the survey region at different measurement times. If limited SVPs or only a surface sound velocity are adopted, significant equivalent SVP errors will be brought to the calculation of measurement distances between the vessel-mounted transducer and the underwater transponder, and thus influences the final positioning accuracies of seafloor control points [5]; (3) the operation is time consuming and

✉ Yajing Zou
914580788@qq.com

1 School of Geodesy and Geomatics, Wuhan University, 129 Luoyu Road, Wuhan 430079, Hubei, China

2 School of Power and Mechanical Engineering, Wuhan University, Wuhan 430072, Hubei, China

3 The First Institute of Oceanography, SOA, Qingdao 266061, Shandong, China

4 BGP INC, China National Petroleum Cooperation, Zhuozhou 072751, Hebei, China

labor intensive. In four-leaf method, a repeat depth sounding operation is demanded to seek an average depth and the vertical coordinate of a seafloor control point is obtained by combing the average depth with the tide level. Moreover, vessel attitudes change with the model error of tide level, wind wave and vessel manipulation, which also bring errors to the absolute vertical datum transfer [6–8].

With the development of underwater acoustic positioning technology and equipment, the transponders installed on the seafloor control points can measure mutually the distances between each other. Because the transponders are arranged approximately in an isothermal layer, both the elevation differences and the differences of sound velocity between them are small, which means the accuracies of measurement distances between the control points are relatively high. Moreover, if the absolute datum transfers are carried out at several control points, the absolute coordinates of other control points can be obtained by constraint adjustment combined with these measurement distances among all the control points.

The process of mutually measuring distances between underwater transponders can improve the accuracy and efficiency of seafloor control network measurement significantly, but the traditional method is still required for the absolute datum transfer of above individual control points.

To improve the accuracy and efficiency of absolute datum transfer in seafloor control network, a new method, based on sailing circle of survey vessel around the underwater transponder and independent of sound velocity profiles (SVPs), is put forward. This method is defined as sailing-circle positioning method and introduced below in detail.

2 Improved intersection positioning model

In the process of acoustic positioning, if one way propagation time of acoustic wave from vessel-mounted transducer to seafloor transponder (control point) is t_i, measurement distance is ρ_i, the coordinates of transducer are $\mathbf{x_i}$, the coordinates of transponder are $\mathbf{x}$, then the observation equation can be depicted as Eq. 1:

$$\rho_i = f(\mathbf{x_i}, \mathbf{x}) + \delta\rho_{vi} + \delta\rho_{ti} + \varepsilon_i \tag{1}$$

where $f(x_i, x) = \|\mathbf{x_i} - \mathbf{x}\|^2$ which is the secondary module of $\mathbf{x_i} - \mathbf{x}$ and stands for the geometrical distance between transducer and transponder; $\delta\rho_{vi}$ is the ranging error caused by sound velocity error, namely the equivalent SVP error; $\delta\rho_{ti}$ is the ranging error caused by time delay error, namely the equivalent time delay error; ε_i is the random error.

Eq. 1 can be linearized as Eq. 2:

$$\delta\rho_i - \delta\rho_{si} = \mathbf{b_i}\mathbf{dx} + \varepsilon_i \tag{2}$$

where $\delta\rho_i = \rho_i - f(x_i, x)$; $\delta\rho_{si}$ is the system error and depicted as $\delta\rho_{si} = \delta\rho_{vi} + \delta\rho_{ti}$; $\mathbf{dx}$ are the coordinate corrections of the transponder; $b_i = (\cos\alpha_i\sin\theta_i, \sin\alpha_i\sin\theta_i, \cos\theta_i)$ and b_i is a unit vector of $f(x_i, x)$ in the transducer coordinate system (TCS); θ_i is the included angle between $f(x_i, x)$ and the vertical direction, and α_i is the included angle between y axis and the projection of $f(x_i, x)$ in the horizontal plane.

If multiple distances are measured between the transducer and the transponder, multiple equations can be constructed as Eq. 2, and the matrix form of these equations is depicted as Eq. 3:

$$\mathbf{V} = \mathbf{Bdx} + \mathbf{d\delta\rho} - \mathbf{\delta\rho} \tag{3}$$

where $\mathbf{dx} = \mathbf{x} - \mathbf{x_0}$, $\mathbf{d\delta\rho} = \mathbf{\delta\rho_s} - \delta\rho_{s0}$, $\mathbf{x_0}$ are the initial coordinates of underwater transponder and $\delta\rho_{s0}$ is the initial value of system error.

Based on the least squares criterion $\mathbf{V^T P V} = $ min, $\mathbf{x}$ can be solved by the following two models:

2.1 The traditional intersection positioning model

If the equivalent time delay error $\delta\rho_{ti}$ is corrected and the sound ray tracing is implemented in the calculation of measurement distances, then the system error $\mathbf{\delta\rho_s}$ is eliminated and the coordinate corrections $\mathbf{dx}$ can be depicted as Eq. 4:

$$\mathbf{dx} = (\mathbf{B^T P B})^{-1}\mathbf{B^T P\delta\rho} = \mathbf{N}^{-1}\mathbf{B^T P\delta\rho} \tag{4}$$

Multiple iterations are required until $\|\mathbf{dx}\|^2$ is less than a given tolerance. The absolute coordinates of seafloor control point are obtained finally by Eq. 5:

$$\mathbf{x} = \mathbf{x_0} + \mathbf{dx} \tag{5}$$

The positioning accuracy of the control point can be evaluated by Eq. 7:

$$\hat{\sigma}_0 = \sqrt{\frac{\mathbf{V^T P V}}{n-3}} \tag{6}$$

$$\hat{\sigma}_x = \hat{\sigma}_0\sqrt{tr(\mathbf{B^T P B})^{-1}} = \hat{\sigma}_0\sqrt{tr(\mathbf{N})^{-1}} \tag{7}$$

2.2 The improved intersection positioning model

If the equivalent time delay error $\delta\rho_{ti}$ is corrected but the sound ray tracing is not implemented in the calculation of measurement distances, based on the impact of sound velocity on the measurement distances, the equivalent SVP error can be considered as a constant and estimated when incident angles of these measurement distances are changeless [9]. The coefficient matrix changes from $\mathbf{B}$ to $\mathbf{F}$ as Eq. 8:

$$\mathbf{F} = [\mathbf{B} \quad \mathbf{j_n}], \quad \mathbf{j_n} = [1 \quad 1 \quad \dots \quad 1]^{\mathrm{T}} \tag{8}$$

The unknown parameters can be solved by Eq. 9:

$$\left[\mathbf{dx^T} \quad \mathrm{d}\delta\rho\right]^{\mathrm{T}} = (\mathbf{F^T P F})^{-1} \mathbf{F^T P} \delta\boldsymbol{\rho} \tag{9}$$

Similarly, multiple iterations are required to correct measurement distances and coordinates until $\|\mathbf{dx}\|^2$ is less than the tolerance, then the absolute coordinates of seafloor control point are determined.

In contrast to the traditional intersection positioning model, the improved model does not need SVP in the data processing and thus simplifies the measurement of absolute datum transfer.

3 Measuring method for absolute datum transfer

3.1 Sailing-circle positioning

If the measurement distances between the seafloor control points and the vessel-mounted transducer are processed by sound ray tracing method, and the time delay error is corrected, then the effects of system error $\delta\rho_s$ are eliminated, and the accuracies of measurement distances can be considered as equal, which means the weight matrix $\mathbf{P}$ can be considered as a unit matrix. The GDOP of spatial geometric figure can be obtained by Eq. 10 [10–12]. The geometric figure is used to determine the coordinates of control points by intersection positioning.

$$\mathrm{GDOP} = \sqrt{\mathrm{tr}\left[(\mathbf{B^T P B})^{-1}\right]} = \sqrt{\mathrm{tr}\left[(\mathbf{B^T B})^{-1}\right]} = \sqrt{\mathrm{tr}(\mathbf{N}^{-1})} \tag{10}$$

In Eq. 10, the matrix $\mathbf{N}$ is depicted as Eq. 11:

$$\mathbf{N} = \mathbf{B^T B} = \begin{bmatrix} \sum_{i=1}^{n} \cos^2\alpha_i \sin^2\theta_i & \sum_{i=1}^{n} \cos\alpha_i \sin\alpha_i \sin^2\theta_i & \sum_{i=1}^{n} i\cos\alpha_i \sin\theta_i \cos\theta_i \\ \sum_{i=1}^{n} \cos\alpha_i \sin\alpha_i \sin^2\theta_i & \sum_{i=1}^{n} \sin^2\alpha_i \sin^2\theta_i & \sum_{i=1}^{n} \sin\alpha_i \sin\theta_i \cos\theta_i \\ \sum_{i=1}^{n} \cos\alpha_i \sin\theta_i \cos\theta_i & \sum_{i=1}^{n} \sin\alpha_i \sin\theta_i \cos\theta_i & \sum_{i=1}^{n} \cos^2\theta_i \end{bmatrix} \tag{11}$$

As $\mathbf{b_i}$ in Eq. 2 is a unit vector, it can be known that the trace of $\mathbf{N}$ is equal to the number of unit vectors by matrix properties, which can be depicted as Eq. 12:

$$\mathrm{tr}(\mathbf{N}) = \sum_{i=1}^{3} \lambda_i = \mathrm{tr}\left[(\mathbf{B^T B})\right] = \mathrm{tr}\left[(\mathbf{B B^T})\right] = n \tag{12}$$

where λ_i is the eigenvalue of the matrix $\mathbf{N}$. The trace of $\mathbf{N}$'s inverse matrix is obtained by Eq. 13.

$$\mathrm{tr}(\mathbf{N}^{-1}) = \sum_{i=1}^{3} \frac{1}{\lambda_i} \geq 3\sqrt[3]{\frac{1}{\lambda_1 \lambda_2 \lambda_3}} \geq 9 \Big/ \sum_{i=1}^{3} \lambda_i = 9/n \tag{13}$$

Only if $\lambda_1 = \lambda_2 = \lambda_3 = n/3$, Eq. 13 takes equal and the GDOP achieves the minimum. Then, $\mathbf{N}$ must satisfy Eq. 14:

$$\mathbf{N} = \mathbf{B^T B} = \frac{n}{3}\mathbf{I} \tag{14}$$

where $\mathbf{I}$ is a unit matrix.

When the GDOP is the lowest, the positioning accuracy of seafloor control point is the highest. According to Eq. 14, to guaranty the highest positioning accuracy, the figure formed by track points needs to satisfy the following conditions in Eq. 15:

$$\mathrm{Condition\ 1}: \sum_{i=1}^{n} \cos\alpha_i \sin\alpha_i \sin^2\theta_i = \sum_{i=1}^{n} \cos\alpha_i \sin\theta_i \cos\theta$$

$$= \sum_{i=1}^{n} \sin\alpha_i \sin\theta_i \cos\theta = 0$$

$$\mathrm{Condition\ 2}: \sum_{i=1}^{n} \cos^2\alpha_i \sin^2\theta_i = \sum_{i=1}^{n} \sin^2\alpha_i \sin^2\theta$$

$$= \sum_{i=1}^{n} \cos^2\theta = \frac{n}{3} \tag{15}$$

It is easy to demonstrate that the Condition 1 can be satisfied when n track points on water surface around the underwater control point form an n-regular polygon with the circumradius of r.

The conclusion can be proved as below.

The horizontal azimuths of the track points can be expressed by Eq. 16.

$$\alpha_i = (i-1)\beta, \quad \beta = 2\pi/n \tag{16}$$

The sum of sine, cosine, and product of sine and cosine can be depicted as Eq. 17 [13, 14]:

$$\sum_{i=1}^{n} \cos\alpha_i = \sum_{i=1}^{n} \sin\alpha_i = \sum_{i=1}^{n} \sin\alpha_i \cos\alpha_i = 0 \tag{17}$$

If the depth difference between the vessel-mounted transducer and the underwater transponder is h, the cosine

of angle θ_i between the geometrical distance $f(x_i, x)$ and the vertical direction can be obtained by Eq. 18:

$$\cos \theta_i = \frac{h}{\sqrt{h^2 + r^2}} \qquad (18)$$

Then, the matrix $\mathbf{N}$ can be simplified by Eq. 19:

$$\mathbf{N}(n) = \mathrm{diag}\left(\frac{nr^2}{2(h^2 + r^2)}, \frac{nr^2}{2(h^2 + r^2)}, \frac{nh^2}{h^2 + r^2}\right) \qquad (19)$$

Equation 19 shows that an n-regular polygon with arbitrary radius formed by n track points meets the Condition 1 in Eq. 15.

According to Eq. 10, when the depth of h and the circumradius of r are known, the GDOP of the figure constructed by the n-regular polygon and the underwater transponder can be described as the function of the plane position (x, y). With the help of the simulation experiments, it is generalized that when $(x, y) = (0, 0)$, which means the underwater transponder is under the center of n-regular polygon, the GDOP is the lowest.

Figure 1 shows the changes of GDOPs with the underwater transponder positions in the n-regular polygon when $h = 80$ m and $r = 100$ m. Figure 1a–c shows the changes, respectively, when track points on water surface form a square, a regular pentagon, and a regular hexagon. It is observed that when the underwater transponder is under the center of n-regular polygon, the GDOP is the lowest, that is to say when the n track points form an n-regular polygon around the projection of underwater control point, the positioning accuracy of underwater control point is the highest.

Furthermore, we can superpose an n_1-regular polygon and an n_2-regular polygon with the same circumradius of r. As the matrix $\mathbf{N}$ of both regular polygons meets Eq. 19, $\mathbf{N}$ of the superposed figure also meets that, which can be proved as Eq. 20:
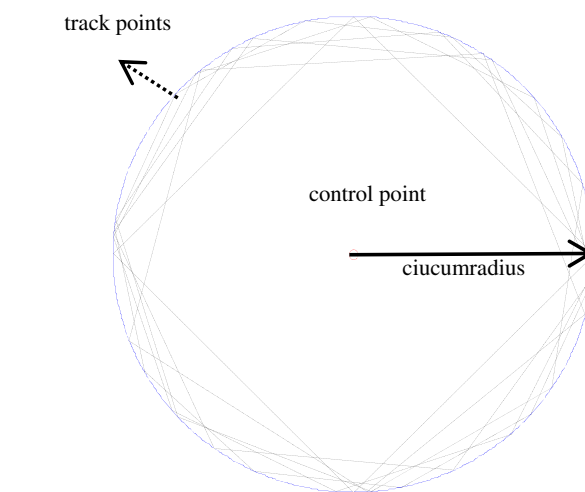

Fig. 2 The circle formed by superposing multiple regular *polygons*: the *red point* stands for the control point; the regular polygons are constructed by *dash lines* between track points

$$\mathbf{B^T B} = \mathbf{B_1^T B_1} + \mathbf{B_2^T B_2} = \mathbf{N}(n_1) + \mathbf{N}(n_2) = \mathbf{N}(n_1 + n_2) \qquad (20)$$

It means that when the number of track points is $n_1 + n_2$ and the figure of these points is formed by superposing an n_1-regular polygon and an n_2-regular polygon with the same circumradius, the GDOP of this figure will also be the lowest. Similarly, the figure formed by superposing all of regular polygons with the same circumradius can also obtain the lowest GDOP. And if the number of regular polygons is enough, the formed figure can be approximated to a circle as shown in Fig. 2. It means that the positioning accuracy of the seafloor control point will be the highest if the survey vessel sails along a circle around the control point, which indicates the superiority of sailing-circle positioning method.
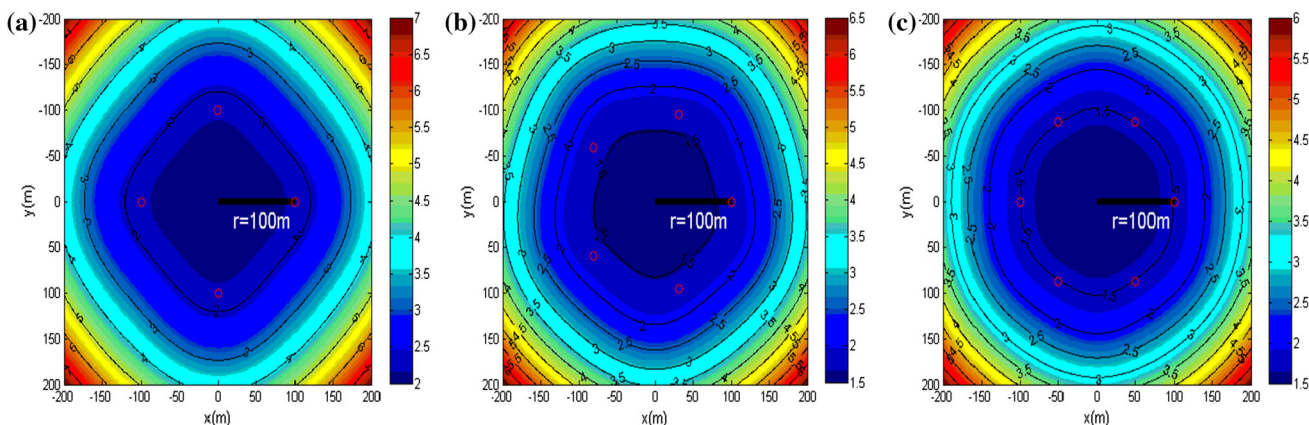

Fig. 1 The changes of GDOPs of underwater transponder in different position when track points form regular *polygons*: **a** the changes when points form a *square*; **b** the changes when points form a regular *pentagon*; **c** the changes when points form a regular *hexagon*

3.2 Determination of the sailing radius

When the survey vessel sails around the seafloor control point along a circle, the GDOP can be influenced by the radius r of the sailing circle. According to Eq. 19, the GDOP is depicted as the function of r in Eq. 21:

$$\text{GDOP} = g(r) = \sqrt{(r^2 + h^2)/nh^2 + 4(r^2 + h^2)/nr^2} \quad (21)$$

Take the derivative of GDOP with respect to r and we can get the lowest GDOP and the optimum radius $r = 1.414\,h$. Substitute $r = 1.414\,h$ into Eq. 19 and we can find it satisfies the Condition 2 in Eq. 15 which further supports the conclusion of the optimum radius $r = 1.414\,h$. If the number of track points is $n = 10$, and the scale factor is $w = r/h$, then the changes of GDOPs with w are shown in Fig. 3a.

If the equivalent SVP errors of the measurement distances are not corrected, the ranging accuracies would be proportional to the distances. Under this situation, the lowest GDOP cannot guarantee the highest positioning accuracy of the transponder or seafloor control point.

$$\sigma_x = \sigma_0 \text{GDOP} \quad (22)$$

$$\sigma_0 = \sqrt{\rho}\,\sigma_{km} = \sqrt[4]{r^2 + h^2}\,\sigma_{km} \quad (23)$$

In Eq. 23, σ_0 is the prior measurement accuracy, and σ_{km} is the mean square error of 1 km measurement distance. According to Eq. 22, the prior positioning accuracy of underwater transponder can be depicted as the function of r in Eq. 24.

$$\sigma_x = \sigma_0 \text{GDOP}$$
$$= \sigma_{km}\sqrt{(r^2 + h^2)^{3/2}/nh^2 + 4(r^2 + h^2)^{3/2}/nr^2} \quad (24)$$

Take the derivative of σ_x with respect to r, we can get the highest accuracy and the optimum radius $r = 1.045\,h$. If the water depth is $h = 100$ m, $\sigma_{km} = 1$ m, and the number of track points is $n = 10$, then the changes of positioning accuracies with w are shown in Fig. 3b.

In conclusion, if the time delay errors are corrected, and measurement distances are processed by sound ray tracing method with the aid of SVP, that is to say the system errors are corrected effectively, then the ranging accuracies of each distances can be considered as equal and the positioning accuracy will be the highest when the sailing radius $r = 1.414\,h$. Otherwise, if system errors of each distances are not corrected effectively, the positioning accuracy will be the highest when the sailing radius is $r = 1.045\,h$.

4 Correlation between the accuracy of the datum transfer and SVP

If the survey vessel sails along a circle with radius r around the underwater control point on the sea surface, n track points are selected at equal spacing, one way propagation time of acoustic wave from vessel-mounted transducer to seafloor transponder (control point) is t_i, the equivalent time delay error of transponder is corrected ($\delta\rho_{ti} = 0$), then the measurement distance can be depicted as $\rho_i = ct_i$ where c is the surface sound velocity. Because only the surface velocity is taken into consideration, the equivalent SVP error $\delta\rho_{vi} = \Delta c_i t_i$ will be brought into ρ_i. Because the incident angles of ρ_i are equal when the vessel sails along a circle, according to the sound ray tracing method, the equivalent SVP error $\delta\rho_{vi}$ of measurement distance ρ_i can
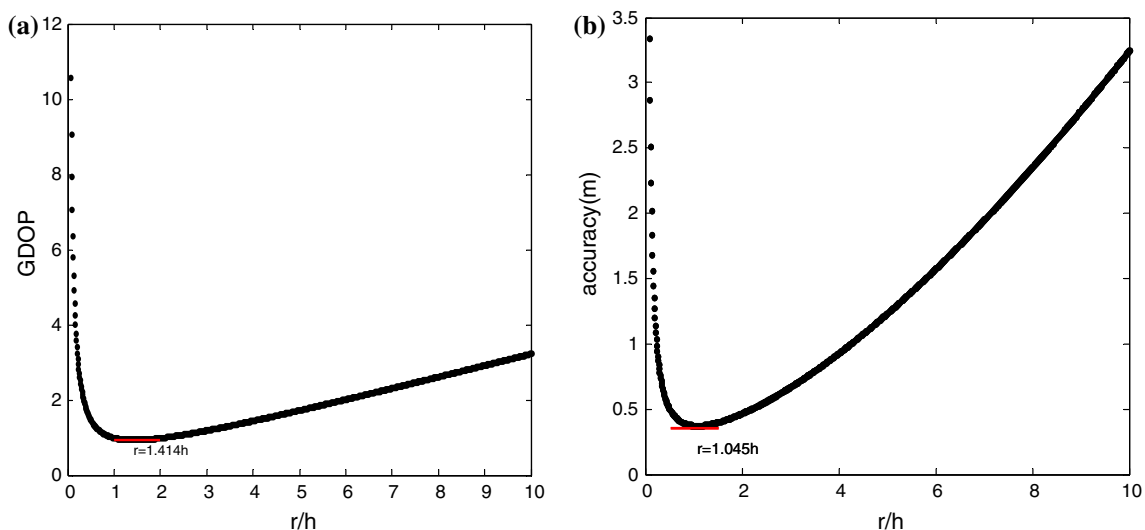

Fig. 3 The changes of GDOPs and prior positioning accuracies with the scale factor: **a** the changes of GDOPs when the sound velocity error is eliminated; **b** the changes of prior positioning accuracies when the sound velocity error is not eliminated

be considered as equal and depicted as $\delta\rho_{vi} = \delta\rho_{v0}$. According to Eq. 9, the impact $\mathbf{dx_v}$ of $\delta\rho_{vi}$ on the coordinates of seafloor control point is depicted as Eq. 25:

$$\mathbf{dx_v} = (\mathbf{B^T P B})^{-1}\mathbf{B^T P}\delta\boldsymbol{\rho_v}, \delta\boldsymbol{\rho_v} = \mathbf{j_n}\delta\rho_{v0} \tag{25}$$

Because the ranging accuracies of the measurement distances are approximately equal, the weight matrix $\mathbf{P}$ can be considered as a unit matrix. Because the track points are selected at equal spacing, matrix $\mathbf{N}$ can be calculated by Eq. 19. Then, Eq. 25 can be simplified as Eq. 26.

According to Eq. 26, if the sailing-circle positioning method is applied, the horizontal coordinates (x, y) of the seafloor transponder will not be influenced by the equivalent SVP error, but z coordinate will be influenced and the influence will be proportional to the equivalent SVP error $\delta\rho_{v0}$. Equation 26 indicates that if z coordinate is provided by an accurate interior pressure sensor or only horizontal coordinates (x, y) are required, a surface sound velocity instead of SVPs is enough to determine the accurate coordinates of control point.

5.1 Experiment in Songhua lake

The depth of the experiment region is about 60 m in Songhua lake. The underwater terrain of experiment region is relatively flat as shown in Fig. 4a. Five transponders (underwater control points) marked as C2, C4, C5, C6, and C8, were set on the lakebed and distributed in the water region within the scope of 134 m × 102 m as shown in Fig. 4b. To get an accurate measurement distance, the sound velocity profiles (SVPs) were measured at the beginning, the middle and the end of the datum transfer. Figure 4c shows the SVP measured at the middle of the experiment, which denotes that an obvious inflection point appears at the water depth of 40 m and the significant sound velocity difference of 40 m/s exists in the experimental region with only 60 m water depth. Besides, the coordinates of vessel-mounted transducer and the antenna center of GPS RTK were strictly measured in the vessel frame system (VFS), which would be used for the subsequent calculation of absolute geographic coordinates of the vessel-mounted

$$\mathbf{dx_v} = \mathbf{N^{-1}B^T}\delta\boldsymbol{\rho_v}$$

$$= \begin{bmatrix} \dfrac{2(h^2+r^2)}{nr^2} & 0 & 0 \\ 0 & \dfrac{2(h^2+r^2)}{nr^2} & 0 \\ 0 & 0 & \dfrac{h^2+r^2}{nh^2} \end{bmatrix} \begin{bmatrix} \dfrac{r\cos\alpha_1}{\sqrt{h^2+r^2}} & \dfrac{r\cos\alpha_2}{\sqrt{h^2+r^2}} & \cdots & \dfrac{r\cos\alpha_n}{\sqrt{h^2+r^2}} \\ \dfrac{r\sin\alpha_1}{\sqrt{h^2+r^2}} & \dfrac{r\cos\alpha_2}{\sqrt{h^2+r^2}} & \cdots & \dfrac{r\cos\alpha_n}{\sqrt{h^2+r^2}} \\ \dfrac{h}{\sqrt{h^2+r^2}} & \dfrac{h}{\sqrt{h^2+r^2}} & \cdots & \dfrac{h}{\sqrt{h^2+r^2}} \end{bmatrix} \begin{bmatrix} \delta\rho_{v0} \\ \delta\rho_{v0} \\ \cdots \\ \delta\rho_{v0} \end{bmatrix}$$

$$= \begin{bmatrix} \dfrac{2\sqrt{h^2+r^2}\cos\alpha_1}{nr} & \dfrac{2\sqrt{h^2+r^2}\cos\alpha_2}{nr} & \cdots & \dfrac{2\sqrt{h^2+r^2}\cos\alpha_n}{nr} \\ \dfrac{2\sqrt{h^2+r^2}\sin\alpha_1}{nr} & \dfrac{2\sqrt{h^2+r^2}\sin\alpha_2}{nr} & \cdots & \dfrac{2\sqrt{h^2+r^2}\sin\alpha_n}{nr} \\ \dfrac{\sqrt{h^2+r^2}}{nh} & \dfrac{\sqrt{h^2+r^2}}{nh} & \cdots & \dfrac{\sqrt{h^2+r^2}}{nh} \end{bmatrix} \begin{bmatrix} \delta\rho_{v0} \\ \delta\rho_{v0} \\ \cdots \\ \delta\rho_{v0} \end{bmatrix}$$

$$= \begin{bmatrix} \dfrac{2\sqrt{h^2+r^2}\sum\limits_{i=1}^{n}\cos\alpha_i}{nr}\delta\rho_{v0} & \dfrac{2\sqrt{h^2+r^2}\sum\limits_{i=1}^{n}\sin\alpha_i}{nr}\delta\rho_{v0} & \dfrac{\sqrt{h^2+r^2}}{h}\delta\rho_{v0} \end{bmatrix}^T$$

$$= \begin{bmatrix} 0 & 0 & \dfrac{\sqrt{h^2+r^2}}{h}\delta\rho_{v0} \end{bmatrix}^T \tag{26}$$

5 Experiments and analysis

To test the validity and accuracy of the sailing-circle positioning method for absolute datum transfer, the experiments were carried out, respectively, in Songhua lake and South China sea. The two experiments will be depicted in detail as below.

transducer. Moreover, the time delay errors of the 5 underwater transponders were also measured by external instruments and will be used for the accurate calculation of propagation times of the sound wave from the vessel-mounted transducer to the underwater transponders. The traditional method and the sailing-circle positioning method were adopted in the absolute datum transfer, respectively.
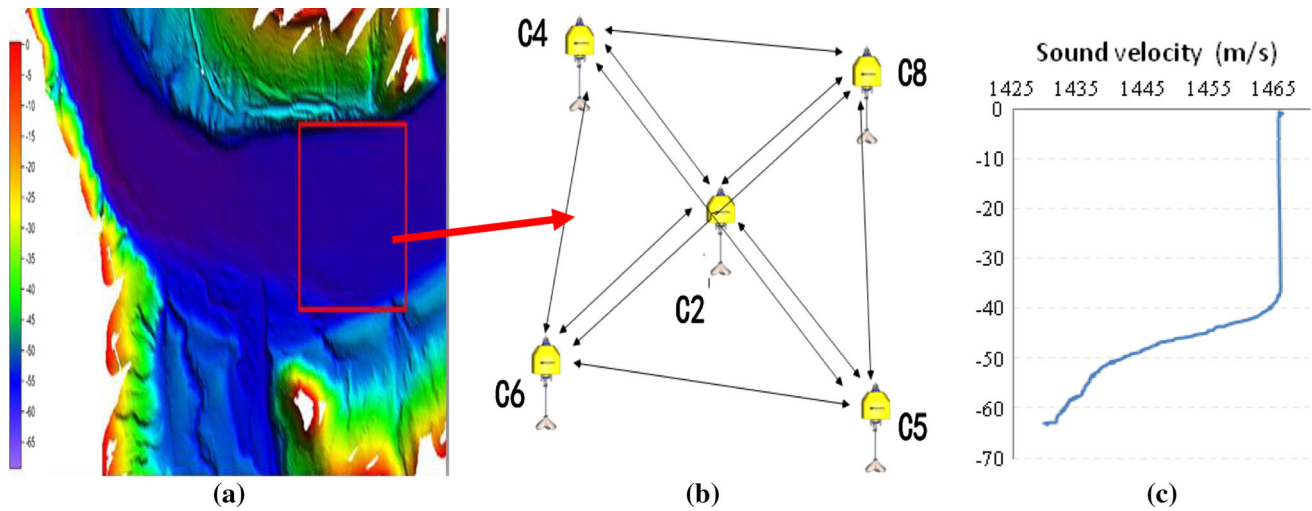
Fig. 4 Experiment in Songhua lake: **a** the experiment region; **b** the distribution of lakebed transponders; **c** SVP
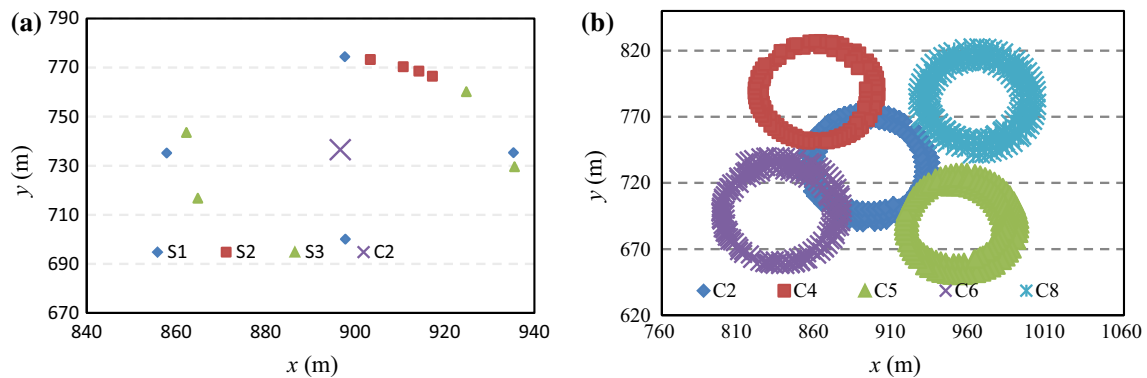

Fig. 5 Experiments finished by the traditional method and the sailing-circle positioning method: **a** the distribution of the vessels and transponder in three sets of traditional measurements; **b** the sailing circles around C2, C4, C5, C6, and C8

Table 1 The coordinates and accuracies of C2 determined by three sets of traditional measurements

Transponder	Set	x (m)	y (m)	z (m)	dx (m)	dy (m)	dz (m)	dz/60 (%)	GDOP
C2	S1	896.60	736.58	60.38	−0.07	0.07	0.01	0.02	1.97
	S2	892.81	728.07	53.74	−3.86	−8.44	−6.63	−11.06	152.01
	S3	897.71	735.41	60.40	1.04	−1.10	0.03	0.05	2.68

By the traditional method, three sets of measurements (namely S1, S2, and S3) were carried out with the help of 4 survey vessels around seafloor control point C2. The distribution of survey vessels and C2 is shown in Fig. 5a. By the sailing-circle positioning method, one vessel sailed around the different seafloor control points along 5 circles with radius of 30 m as shown in Fig. 5b.

In the processing of measurement data by traditional method, first, the measurement distances between mounted-vessel transducers and C2 are processed by sound ray tracing method with the aid of SVP, then the initial horizontal coordinates of C2 are set as the average of the horizontal coordinates of four survey vessels and the initial z coordinate is set as 60 m, finally, the absolute coordinates of C2 can be obtained by multiple iterations of coordinate corrections in Eq. 4. The coordinates of C2 calculated by three sets of measurement data are shown in Table 1, and compared with the real horizontal coordinates provided by RTK when delivering C2 and the real z coordinate provided by an accurate pressure sensor. Then, the positioning errors (dx, dy, dz) and the relative depth errors dz/60 by three sets of measurement data can be calculated.

As shown in Table 1, the positioning accuracy in S1 is the highest, followed by that in S3, and the accuracy in S2

is the lowest. It can be seen in Fig. 5a that four survey vessels in S1 are distributed symmetrically around C2, while in S3 distributed around the C2 asymmetrically and in S2 distributed on one side of C2. The results mean that for absolute datum transfer, the spatial distribution of measuring distances or GDOP (geometric dilution of precision) is very important for positioning accuracy.

The following three methods are applied to the processing of sailing-circle measurement data and the calculation of the coordinates of each underwater control points.

Method 1: With the help of SVP and one way propagation time of acoustic wave, all the measurement distances are processed by sound ray tracing method. Then, the coordinates $(0, y, z)$ of underwater transponder are obtained in the transducer coordinate system, and the geometric distance ρ between the transducer and the transponder is determined as the square root of $y^2 + z^2$. Finally, the coordinates of underwater transponder are calculated by Eq. 4.

Method 2: The measurement distance ρ is directly set as the product of the surface velocity and the propagation time, and then the coordinates of underwater transponder are calculated by Eq. 4.

Method 3: The initial distance ρ is calculated by the product of the surface velocity and the propagation time and is considered as an observation. The equivalent SVP error $\delta\rho_v$ and the coordinates of underwater transponder

are considered as unknown parameters and calculated by Eq. 9. And then ρ is compensated by the equivalent SVP error $\delta\rho_v$. Finally, the coordinates of control point are obtained after multiple iterations until the tolerance is satisfied.

To compare the traditional method with the sailing-circle positioning method, four observations are extracted at equal spacing from the sailing-circle measurement data of C2, and then the coordinates of C2 are solved by the above three methods. The positioning results and accuracies of the three methods are shown in Table 2. Compared with Table 1, the positioning accuracies of the three methods are similar to that in S1 and higher than those in S2 and S3. It shows that only when the survey vessels are distributed symmetrically in the traditional measurement, the sailing-circle positioning method has the similar accuracy with the traditional method. Otherwise, the former has higher accuracy than the latter.

Apply the three sailing-circle positioning method to the calculation of the coordinates of five control points with all track points and the results are shown in Table 3. Because the measurement distances are distributed symmetrically around control points and processed by sound ray tracing method with the help of SVP strictly in Method 1, the positioning accuracy is relatively higher, and the coordinates of control points determined by Method 1 can be taken as reference. The positioning errors are obtained by

Table 2 The coordinates and accuracies of C2 calculated by different methods with four track points

Transponder	GDOP	Method	x (m)	y (m)	z (m)	dx (m)	dy (m)	dz (m)	dz/60 (%)
C2	1.83	1	896.64	736.55	60.39	−0.03	0.04	0.02	0.03
		2	896.64	736.56	60.41	−0.03	0.05	0.04	0.07
		3	896.64	736.55	60.40	−0.03	0.04	0.03	0.05

Table 3 The coordinates and accuracies of transponders calculated by different methods

Transponder	GDOP	Method	x (m)	y (m)	z (m)	dx (m)	dy (m)	dz (m)	dz/60 (%)
C2	0.42	1	896.67	736.51	60.37	–	–	–	–
		2	896.67	736.52	60.46	0.01	0.01	0.09	0.15
		3	896.67	736.52	60.41	0.01	0.01	0.04	0.07
C4	0.31	1	864.98	792.59	59.75	–	–	–	–
		2	864.98	792.59	59.82	0.01	0.01	0.07	0.12
		3	864.97	792.58	59.74	−0.01	−0.01	−0.01	−0.01
C5	0.30	1	955.09	690.37	60.70	–	–	–	–
		2	955.10	690.37	60.79	0.01	0.00	0.09	0.15
		3	955.10	690.38	60.73	0.01	0.00	0.03	0.04
C6	0.29	1	835.07	697.76	59.88	–	–	–	–
		2	835.07	697.76	59.96	0.00	0.00	0.08	0.13
		3	835.07	697.76	59.92	0.00	0.00	0.04	0.06
C8	0.31	1	969.77	787.18	60.63	–	–	–	–
		2	969.78	787.19	60.72	0.01	0.01	0.09	0.15
		3	969.78	787.18	60.64	0.01	0.00	0.00	0.01

comparing the coordinates determined by Method 2 and Method 3 with those determined by Method 1, and shown in Table 3.

It can be seen in Table 3 as below:

1. The maximum errors of positioning results achieved by Method 2 are 0.01 m in x direction, 0.01 m in y direction and 0.09 m in z direction. It means that even if SVP is not or not strictly considered, the equivalent sound velocity error will not influence the horizontal positioning accuracy obviously, but will significantly influence the vertical positioning accuracy.

2. Compared with the positioning accuracy achieved by Method 2, the vertical positioning accuracy achieved by Method 3 is much higher. It means that in the sailing-circle positioning method, it is reasonable to consider the equivalent SVP error as equal and estimate it in adjustment model. Method 3 can not only improve the vertical positioning accuracy, but also improve the transfer efficiency without measuring SVP.

5.2 Experiment in South China sea

A similar experiment was carried out in South China sea. A seafloor transponder was set on the seabed with the depth of approximately 2000 m. The survey vessel sailed around the transponder along 4 circles, respectively, with the radius of 1192, 1957, 2000, and 3357 m. Different sailing circles and SVP are shown in Fig. 6a, b, respectively.

With the help of SVP and propagation time, the measurement data are processed by the above three methods, respectively. The positioning results of different measurement data with different radius are shown in Table 4. Similarly, the coordinates determined by Method 2 and Method 3 are compared with those determined by Method 1, and then the positioning errors (dx, dy, dz) and the relative depth errors $dz/1960$ are shown in Table 4.

As shown in Table 4, the maximum errors of positioning results achieved by Method 2 are 1.14 m in x direction, 0.69 m in y direction and 36.00 m in z direction, while those by Method 3 are 0.90, 0.43 and 4.22 m, respectively.
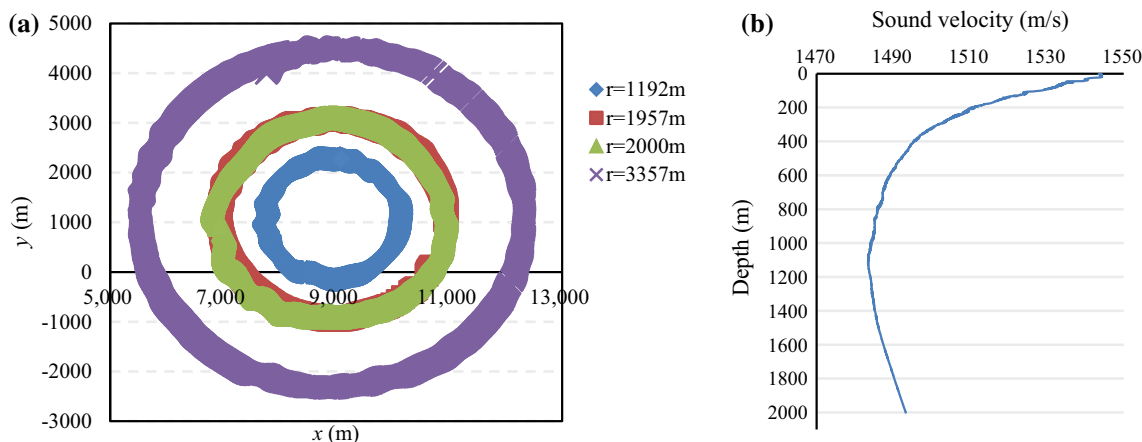

Fig. 6 Experiment in South China sea: **a** sailing circles of the survey vessel around the underwater transponder; **b** SVP in the experiment region

Table 4 The results of different measurement data with different radius calculated by different methods

r (m)	GDOP	Method	x (m)	y (m)	z (m)	dx (m)	dy (m)	dz (m)	$dz/1960$ (%)
1192	0.25	1	8927.26	999.53	1961.26	–	–	–	–
		2	8927.13	998.87	1974.14	−0.14	−0.65	12.89	0.66
		3	8927.23	999.39	1964.14	−0.03	−0.14	2.88	0.15
1957	0.12	1	8927.29	999.28	1960.31	–	–	–	–
		2	8927.16	998.59	1979.26	−0.13	−0.69	18.96	0.97
		3	8927.27	999.17	1963.65	−0.02	−0.11	3.34	0.17
2000	0.12	1	8927.20	998.72	1960.48	–	–	–	–
		2	8927.71	998.56	1977.81	0.51	−0.16	17.33	0.88
		3	8927.61	998.73	1964.32	0.42	0.01	3.84	0.20
3357	0.19	1	8927.08	998.88	1962.48	–	–	–	–
		2	8925.94	998.28	1998.48	−1.14	−0.60	36.00	1.84
		3	8926.18	998.45	1966.58	−0.90	−0.43	4.10	0.21

Table 5 The results of 20 track points extracted from different measurement data with different radius by different methods

r (m)	GDOP	Method	x (m)	y (m)	z (m)	dx (m)	dy (m)	dz (m)	dz/1960 (%)
1192	0.89	1	8928.29	999.90	1961.34	–	–	–	–
		2	8928.21	999.24	1974.24	−0.09	−0.66	12.89	0.66
		3	8928.25	999.60	1964.29	−0.04	−0.30	2.94	0.15
1957	0.70	1	8927.53	999.41	1960.34	–	–	–	–
		2	8927.41	998.73	1979.27	−0.12	−0.68	18.93	0.97
		3	8927.47	999.06	1963.45	−0.06	−0.36	3.12	0.16
2000	0.70	1	8927.60	999.51	1960.99	–	–	–	–
		2	8927.65	999.68	1978.06	0.04	0.17	17.08	0.87
		3	8927.59	999.43	1962.84	−0.02	−0.08	1.85	0.09
3357	0.92	1	8927.18	998.57	1962.36	–	–	–	–
		2	8926.03	997.35	1998.36	−1.15	−1.22	36.00	1.84
		3	8926.46	998.18	1967.18	−0.72	−0.39	4.82	0.25

The above conclusion is verified again that the equivalent SVP error will not influence the horizontal positioning accuracy obviously, but will significantly influence the vertical positioning accuracy. Meanwhile, it is shown that the accuracy of the positioning results calculated by Method 3 is higher than that by Method 2, and Method 3 is more efficient than Method 1 but has the similar accuracy with Method 1.

According to Eq. 26, dz will be proportional to the equivalent SVP error $\delta\rho_v$. In Method 3, the equivalent SVP errors $\delta\rho_{vi}$ are considered equal and corrected, so dz can be weakened. But due to the following reasons, $\delta\rho_{vi}$ are not entirely equal and cannot be corrected exhaustively in the experiment, so there were still 3–4 m error in dz.

1. The experiment area in South China sea is so large that SVPs are changeable and a single SVP cannot represent the change of sound velocity in the experiment area.
2. Because of the impact of the big waves and winds, the track points cannot form a perfect circle and the incident angles of ρ_i are not entirely equal.

In Table 4, the positioning results of sailing-circle measurements with different radius are approximately equal. Through analysis, it is considered that since all the sailing-circle measurement data are involved in the data processing and the calculation of coordinates, the data redundancy increased significantly in the adjustment model, and then the accuracies of final results are improved and the differences between positioning results with different radius are small. To highlight the impact of the sailing radius on the accuracy of datum transfer, 20 observations are extracted at equal spacing from above four sets of sailing-circle measurement data separately, and then the coordinates of control point are solved by the above three methods. The positioning results and accuracies of

different measurement data with different radius and calculated by different methods are shown in Table 5.

As shown in Table 5, the differences between the horizontal coordinates of the same measurement data calculated by different methods are relatively small, while the differences between z coordinates are relatively large. Meanwhile, the positioning accuracy of Method 3 is higher than that of Method 2. The results are consistent with the above conclusion. However, by comparing different positioning results with different sailing radius, we can find that the positioning results with the radius of 1957 and 2000 m are relatively consistent, but the positioning results with the radius of 1192 and 3357 m have difference to some extent and are also different from those with the radius of 1957 and 2000 m. It is analyzed that the value of GDOPs is approximately equal when the sailing radius are 1957 and 2000 m, and the positioning accuracies are relatively higher. It also supports that if the equivalent SVP error is not considered, the positioning accuracy will be higher when the sailing radius r is 1.045 times the depth.

6 Conclusions and recommendations

To overcome the shortcomings of traditional method, the sailing-circle positioning method is put forward in this paper for the absolute datum transfer in building seafloor control network. The proposed method has been verified by the experiments in Songhua lake and South China sea. The following conclusions are also drawn out:

1. The sailing-circle positioning method gives consideration to the symmetry of measurement distances space distribution and the redundancy rate of measurement data in the calculation of point coordinates, and thus improves the positioning accuracy and enhances the operation efficiency relative to the traditional method.

2. If equivalent SVP error of measurement distance is corrected, the positioning accuracy is highest when the sailing radius is 1.414 times the depth of transponder; otherwise, the positioning accuracy is highest when the sailing radius is 1.045 times the depth.

3. In the sailing-circle positioning method, a surface sound velocity instead of SVPs is used for the calculation of measurement distance. The impact of equivalent SVP error on horizontal coordinates is small while that on z coordinate is relatively large. If the equivalent SVP error is considered as an unknown parameter in the adjustment model, the impact can be effectively weakened, and the accuracy of absolute datum transfer can be improved significantly. Furthermore, SVPs are not demanded to measure in this method which can simplify significantly the traditional method.

References

1. Arabelos D, Tscherning CC (2001) Improvements in height datum transfer expected from the GOCE mission. J Geod 75(5–6):308–312

2. Li ZL, Zhang RH, Peng ZH et al (2004) Anomalous sound propagation due to the horizontal variation of seabed acoustic properties. Sci China (Ser G Phys Mech Astron) 47(5):571–580

3. Averbakh VS, Bogolyubov BN, Dubovoi YA et al (2001) Application of hydroacoustic radiators for the generation of seismic waves. Acoust Phys 48(2):121–127

4. Candy JV, Sullivan EJ (1993) Sound velocity profile estimation: a system theoretic approach. Ocean Eng IEEE J 18(3):240–252

5. Zhang ML, Huang MY, Feng HH (2010) Iteration algorithm of revising sound velocity for long baseline acoustic positioning system. Tech Acoust 3:253–257

6. Sun H, Tan DKP, Lu Y (2003) Design and implementation of an experimental GSM based passive radar. In: Radar Conference, proceedings of the international, pp 418–422

7. Liu Y, Li XR (2010) Aided strap down inertial navigation autonomous underwater vehicles. Conference on signal and data processing of small targets 2010, Orlando, APR 05–08, vol 7698, literature 76981H

8. Napolitano F, Cretollier F, Pelletier H (2005) GAPS, combined USBL + INS + GPS tracking system for fast deployable and high accuracy multiple target positioning. Oceans 2005 Eur 2:1415–1420

9. LeBlanc LR, Middleton FH (1980) An underwater acoustic sound velocity data model. J Acoust Soc Am 67(6):2055–2062

10. Kee C, Parkinson B (1994) Calibration of multipath errors on GPS pseudorange measurements. Salt Lake City. In: Proceedings of the 7th international technical meeting of the Satellite Division of the Institute of Navigation (ION GPS 1994), pp 353–362

11. Yarlagadda R, Ali I, Al-Dhahir N et al (2000) Gps gdop metric. IEEE Proc Radar Sonar Navig 147(5):259–264

12. Xue S, Yang Y (2014) Positioning configurations with the lowest GDOP and their classification. J Geod 89(1):1–23

13. El Ghaoui L, Feron E, Balakrishnan V (1994) Linear matrix inequalities in system and control theory. Society for Industrial and Applied Mathematics, Philadelphia

14. Bracewell RN (1986) The Fourier transform and its applications. McGraw-Hill, New York